Water Science & Technology

Water Science & Technology Vol 87 No 1, 83 doi: 10.2166/wst.2022.411

Extraction of extracellular polymeric substances (EPS) from indigenous bacteria of rare earth tailings and application to removal of thorium ions (Th^{4+})

Jianhong Han[a], Hongyan Li[a], Yi Liu[b], Pai Liu[b], Yi Song[a], Yuting Wang[a], Lianke Zhang[a] and Weida Wang[a,*]

[a] School of Energy and Environment, Inner Mongolia University of Science and Technology, No.7, Alding street, Baotou, Inner Mongolia 014010, China
[b] School of Chemical Engineering and Technology, TianGong University, No. 399, Binshui West Road, Xiqing District, Tianjin 300130, China
*Corresponding author. E-mail: wangweida888@163.com

HL, 0000-0002-1629-693X

ABSTRACT

Thorium, as an important radioactive element, is widely present in nature, and its accompanying environmental pollution is also serious. Extracellular polymeric substances (EPS) are commonly found on the surface of microbial bodies and have strong adsorption capacity for metal ions. In this study, four methods were used to extract EPS from indigenous bacteria of rare earth tailings and to determine the best extraction method. The extracted EPS was applied to treat Th^{4+}, and the changes in functional groups and composition of EPS were investigated. The results showed that the ultrasonic method was more efficient than other methods. The best removal efficiency was observed at pH 3.5, Th^{4+} concentration of 20 mg/L, and EPS dosage of 30 mL at 25 °C. After 9 h, the adsorption process reached equilibrium with a maximum removal efficiency of 75.93% and a maximum theoretical adsorption capacity of 25.96 mg/g. The Th^{4+} removal process was consistent with the Langmuir and Freundlich adsorption isotherms and the kinetic data were consistent with the pseudo-second-order kinetic model, which is mainly based on chemisorption. Amide I and amide II of proteins, C–H from aliphatic, as well as O–H and C = O from carboxylic acid play important roles in the adsorption process.

Key words: adsorption, EPS, extraction methods, thorium ion (Th^{4+})

HIGHLIGHTS

- EPS are extracted from indigenous bacteria of rare earth tailings and it has better polysaccharide content than other EPS extracted from other materials.
- Application of EPS to the treatment of Th^{4+} exhibited better adsorption effects.
- The functional groups of EPS play important role in the adsorption of Th^{4+}.

GRAPHICAL ABSTRACT

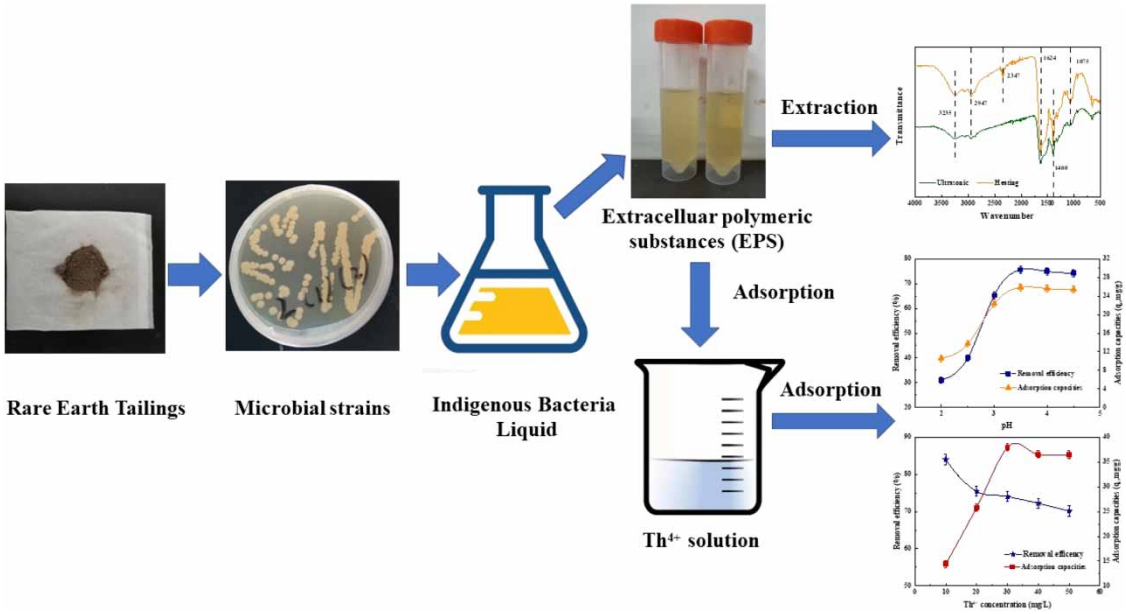

1. INTRODUCTION

Thorium, as a radionuclide, mainly exists in thorium ore, uranium ore and rare earth minerals. In nature, thorium occurs mainly in the form of tetravalent compounds (Th^{4+}). The Bayan Obo rare earth mine in Baotou has the largest thorium content in China, accounting for 77.3% of the total thorium reserves in China (Xu *et al.* 2005; Chen *et al.* 2022). Nowadays, Baotou Bayan Obo rare earth mine has been widely used in energy conservation, environmental protection, green industry, and other low-carbon economic fields. With the popularity of concepts including clean energy, and carbon neutrality, the demand for high-property rare-earth permanent magnetic materials is growing rapidly. The rare-earth permeability is likely to continue to increase.

While rare-earth is fully and efficiently utilized, thorium is not utilized due to its low industrial value, and is often discharged in the form of thorium wastewater, loss, and flying, which not only causes serious pollution to the soil environment around the mining area, but also greatly threatens the safety of groundwater (Xu *et al.* 2005; Chen *et al.* 2022). Thorium is not biodegradable and it tends to accumulate in the human body, causing serious damage (Cadena 1983; Yang *et al.* 2017). Currently, common treatment methods for thorium containing wastewater include adsorption, ion exchange, membrane technologies, solvent extraction, and chemical precipitation (Li *et al.* 2018). Traditional chemical and physical treatment methods have disadvantages such as high cost, complicated operation, and unstable effects. However, adsorption is a simple technique that does not require any special set up and the originality resides in the material itself (Hamane *et al.* 2015). Biosorbents are safe and less polluting to the environment. This is a new heavy metal treatment method that has been proven to have the most potential for development by previous research.

Extracellular polymeric substances (EPS), as a new kind of biological adsorbent, have been widely studied because of their unique advantages in heavy metal adsorption. EPS are high-molecular-weight mixtures that mainly consist of polysaccharides, proteins, humus, fat, nucleic acid, and inorganic substances (Li *et al.* 2018). It is produced, excreted, secreted, and absorbed by cells (mainly bacteria). EPS binds closely with cells and only be extracted by special physical or chemical methods.

In recent years, EPS have been widely applied in various fields such as wastewater treatment, cosmetic industries food, and pharmaceuticals due to their physicochemical and biological properties (Xiao & Zheng 2016). Some studies have shown that EPS extracted from different sources can effectively remove heavy metals (More *et al.* 2014; Nouha *et al.* 2016; Zhao *et al.* 2016). However, the raw materials used to extract EPS in the past are usually only for sludge and bacteria (Wang *et al.* 2014; Gupta & Batul 2016; Wei *et al.* 2016), while the extraction of EPS from indigenous bacteria of rare earth tailings and further

treatment of thorium containing wastewater is relatively little investigated. In this study, indigenous bacteria of rare earth tailings were used to extract EPS and it was applied to the treatment of Th^{4+}, and the optimal extraction method, content, and interaction mechanism of EPS with Th^{4+} were explored.

2. MATERIALS AND METHODS

2.1. Experimental reagent

Anthrone, EDTA, and Coomassie Blue (G-250) were from Sinopharm Chemical Reagent Co., Ltd., HCl from Nanjing Chemical Reagent Co., Ltd., $H_2C_2O_4$ from Fuchen (Tianjin) Chemical Reagent Co., Ltd., $C_{22}H_{18}As_2N_4O_{14}S_2$ and NaOH from Tianjin Chemical Reagent Factory I. H_2SO_4 was from the Beijing Chemical Plant. Bovine serum albumin (BSA) from Tianguangyuan (Xian) Biotechnology Co., Ltd., Glucose from Xilong Scientific Co., Ltd., and $Th(NO_3)_4{\cdot}4H_2O$ was supplied by the Beijing Research Institute of Chemical Metallurgy of China National Nuclear Industry Co.. The reagents used in the experiments were analytically pure. All the solutions in the experiment were made from deionized water.

2.2. Tailings samples

Tailings collected from the rare earth tailings dam in Baotou city, Inner Mongolia autonomous region, China were used in this study. The tailings are washed with water, dried, crushed, and sieved. Of these, tailings with an average diameter of less than 2 mm were used for the following studies.

2.3. Microbial strains

Rare earth tailings samples were used as the source of strains, and the target strains were screened by the diluted plate method. The 1 g of tailings sample was transferred to a conical flask containing 99 mL of sterile saline water and shaken to make a suspension, which was allowed to stand for 1 min. The suspension was diluted in a 10-fold gradient, inoculated on LB solid medium and cultivated for 1–2 d at 32 °C in a constant temperature incubator (Han *et al.* 2020). The most numerous individual colonies on the medium with regular edges and smooth upper surfaces and larger diameters (about 3 mm) were selected and streaked repeatedly on the same solid medium for separation. The target strains were obtained when the colony morphology was consistent on the medium. A bacterial strain, named K-1, was isolated and screened from the tailings sample, and the strain K-1 was sent to Shanghai Meiji Biomedical Technology Co., Ltd for 16S rDNA sequence analysis (Han *et al.* 2020). The ITS sequence was compared with BLAST sequence similarity in the NCBI online database, and it was found that strain K-1 and *Lysinibacillus sp.* strain LJ75 were located in the same branch with 100% similarity, so strain K-1 was identified as Lysinibacillus fusiformis.

2.4. Extraction methods of EPS

In this study, the comparison experiments involved four conventional extraction methods, including, ultrasound, heating, and treatment with NaOH and EDTA. The isolated individual strain K-1 was inoculated into LB liquid medium and proliferated at a constant temperature of 32 °C for 24 h, which was the sample bacteria liquid for EPS extraction. Specific extraction procedures are described in Figure 1.

All the EPS samples were measured immediately to avoid the degradation of EPS during storage. After the extraction, the protein and polysaccharide were quantified, and the concentration of EPS was used to express the sum of the two contents. The concentration of EPS was used to perform unit conversions (Kang *et al.* 2016).

2.5. EPS analysis

The functional groups of EPS were also analyzed by Fourier Transform Infrared spectrometer (FTIR) (BRUKER TensorII, Germany) with a resolution of 4 cm^{-1} and scan a range of 400–4000 cm^{-1}. EPS was freeze dried by a lyophilizer (Alpha 1-2 LDplus, Christ, Germany) before FTIR determination. The EPS before and after adsorption was added to a 1 cm quartz cuvette and placed in the 3D-EEM (HITACHIF4600, Hitachi Limited, Tokyo, Japan) to determine its composition changes. The scanning interval was 5 nm, while the scanning speed was 12,000 nm/min. The infrared and fluorescence spectrum were analyzed by Origin 2018.

The protein contents were determined using the Coomassie Blue method, with bovine serum albumin (BSA) as the standard. The polysaccharide contents were measured using the anthrone-sulfuric acid method, with glucose as the standard.

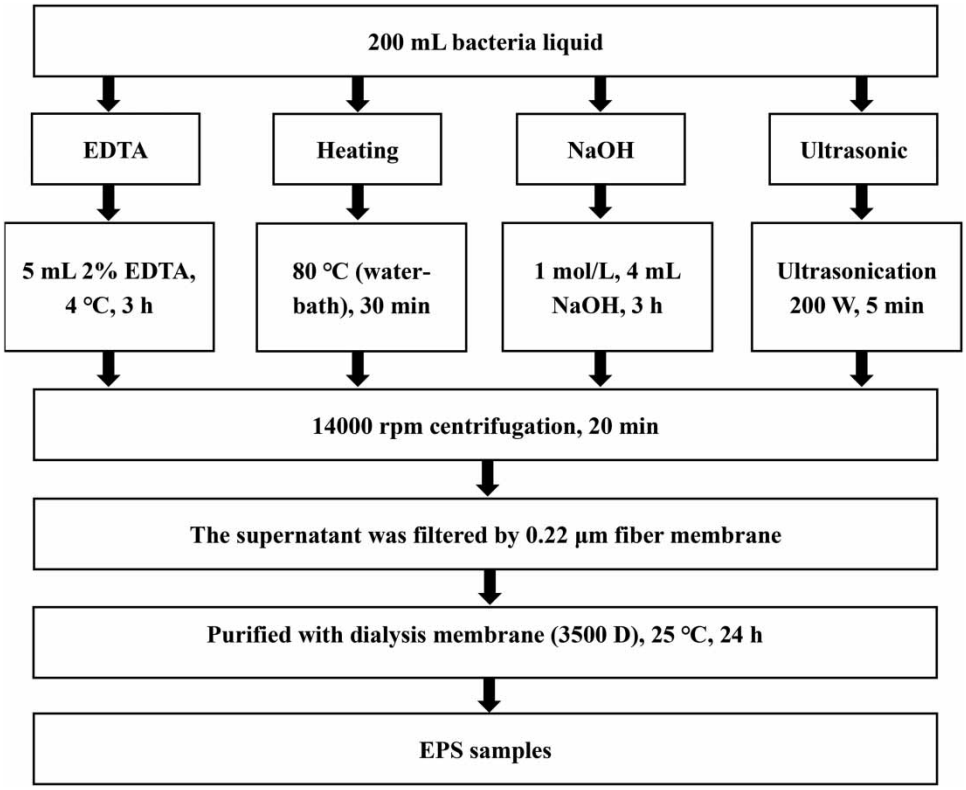

Figure 1 | Four EPS extraction processes.

2.6. Th^{4+} adsorption experiments

The experiments were conducted in 250 mL conical flasks containing 20 mL of Th^{4+} solution at 25 °C. The 30 mL of EPS extracted by different methods were used as adsorbent and placed in dialysis bags and then in conical flasks. The conical flasks were agitated at 150 r/min on a thermostatic oscillator for 15 h, allowing ample time for adsorption equilibrium. To determine the biosorption isotherms, the initial Th^{4+} concentration was varied from 10 to 50 mg/L while the EPS dosage in each experiment was held constant at 30 mL. After 15 h, 1 mL of the solution in the conical flask was taken and added to the 10 mL colorimetric tube and 1 mL of 10% oxalic acid solution was added to the colorimetric tube and shaken well. Then 0.5 mL of 0.05% Arsenazo iii solution was added as the chromogenic agent and finally titrated to the scale line with 7 mol/L HCl, shook well, and stood for 10 min. The residual metal ion concentration (C_e) in the solution was determined by UV-visible spectrophotometer (752N, Shanghai Yidian Analytical Instruments Co., Ltd, China) at 660 nm. The removal efficiency R (%) and adsorption capacities q_e (mg/g) of Th^{4+} by EPS were calculated based on the concentration difference before and after the reaction, as shown in Equations (1) and (2):

$$R = \frac{C_0 - C_e}{C_0} \times 100\% \tag{1}$$

$$q_e = \frac{(C_0 - C_e) \times V}{m} \tag{2}$$

where C_0 and C_e (mg/L) are the initial and equilibrium Th^{4+} concentrations, respectively; V is the volume of the solution, L; m is adsorbent dosage, g.

3. RESULTS AND DISCUSSION

3.1. Comparison of extraction methods of EPS

3.1.1. FTIR spectra of EPS extracted by different methods

FTIR spectra examples of EPS extracted from different methods are presented in Figures 2 and 3. Table 1 recaps the functional groups corresponding to bands observed on FTIR spectra of EPS extracted by different methods. The different functional groups observed in the EPS samples extracted by indigenous bacteria of rare earth tailings are similar to Tang's results (Tang *et al.* 2021).

For EPS extracted by ultrasonic and heating, the same characteristic bands can be observed on every EPS FTIR spectra presented in Figure 2. Bands 3200–1592 cm^{-1} can be attributed to protein and polysaccharide functional groups. Carboxylic groups, under acid or basic salt form, are responsible for some less intense bands and they suggest, when combined with the other observed bands, the presence of uronic acids and of humic substances (Comte *et al.* 2006). The band at 2347 cm^{-1} of EPS FTIR spectrum extracted by the heating method may be caused by sample contamination in the testing process.

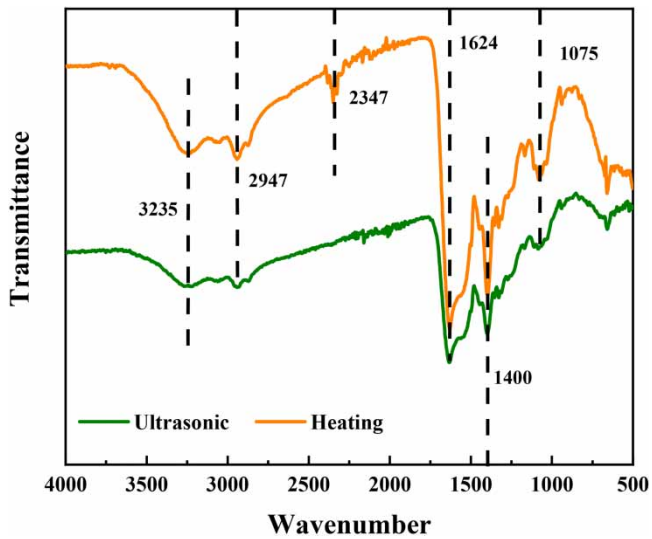

Figure 2 | FTIR spectra of EPS extracted by physical methods.

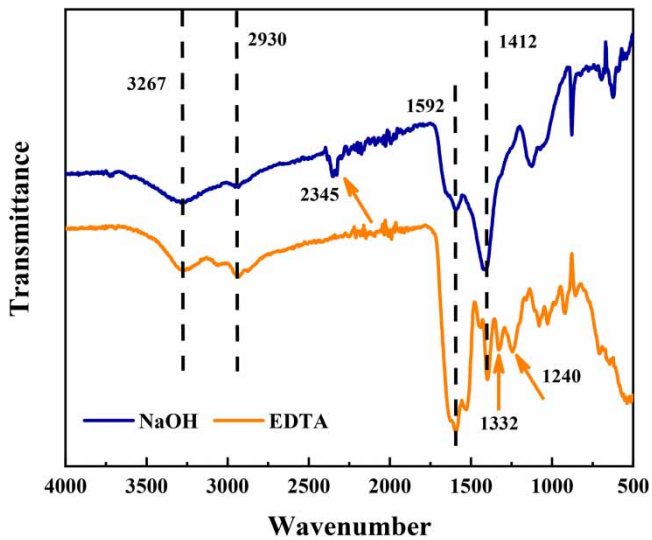

Figure 3 | FTIR spectra of EPS extracted by chemical methods.

Table 1 | Main functional groups observed from FTIR spectra of EPS

Wavenumber	Vibration type and corresponding functional groups
3200–3420	Stretching vibration of O–H groups of carbohydrates and N–H groups of proteins
2900–3000	Stretching vibration of methyl and methylene C–H
1625–1660	Stretching vibration of C = O and C–N (amide I) of proteins
1592	Stretching vibration of C–N and deformation vibration of N–H (amide II) of Proteins (peptidic bond)
1380–1460	Aliphatic C–H bending vibration and stretching vibration of C = O in carboxylates
1235–1245	Stretching vibration of O–H and deformation vibration of C = O of carboxylic acid
1040–1080	Stretching vibrations of C–O–O and C–O, which may be caused by carbohydrate sand aromatics
<1000	Fingerprint region presented the existence of phosphate or sulfur functional groups

The FTIR spectra of EPS extracted by chemical methods (Figure 3) show particular bands which do not appear for EPS extracted by the physical methods. For the FTIR spectrum obtained for EPS extracted by the treatment with EDTA, the bands 1332 and 1240 cm^{-1} are seen to be associated with C–N stretching. Moreover, bands 1592 cm^{-1} are attributed to carboxylate functions. This demonstrates contamination of EPS by the chemical reagent. This is consistent with previous experimental results. The FTIR spectrum obtained for EPS extracted by the NaOH method shows a band at 2345 cm^{-1}. These bands could be interpreted as specific bands for the result of a NaOH and EPS reaction (Comte *et al.* 2006).

3.1.2. Effects of different extraction methods on EPS content

EPS of the indigenous bacteria of rare earth tailings were extracted following the procedures in section 2.4. The quantities of proteins and polysaccharides were measured to represent the EPS yields, as they are the main component of EPS. The experimental results are shown in Table 2. The results show that the content of polysaccharides in EPS extracted from the indigenous bacteria of rare earth tailings was higher than that of protein. This is similar to the research results of Zhang *et al.* (2008). The results indicated that the yields of EPS were highly dependent on the extraction method. The content of total EPS and protein extracted by the ultrasonic method is the highest among the four extracted methods indicating that ultrasonic method is the best method to extract this sample EPS. Thus, all EPS extracted by the ultrasonic method was applied in the subsequent experiments.

As shown in Table 2, the contents of polysaccharides of EPS extracted by ultrasonic method are the highest. This is because the ultrasonic method uses ultrasonic shear force, cavitation, and so on to make EPS off the cell surface into the water. The action intensity is mild, which can effectively separate the effective components of EPS at the same time, but can avoid damaging the effective components of EPS. The content of polysaccharides extracted by heating method was the highest among the four methods. Increasing the temperature will lose the structure of the sample and could decrease van der Waals forces and hydrogen bonding between EPS and cells (Li & Yang 2007; Guo *et al.* 2010; Zhou *et al.* 2016), and extract the firmly bound EPS while the proteins and polysaccharides in EPS can be hydrolyzed in the extraction process. In Table 2, the biochemical composition content was lower in the EPS extracted by treatment with NaOH than in other methods. The addition of NaOH solution caused the groups, such as carboxylic groups, to be ionized, resulting in a strong repulsion and then separation between the EPS and the cells, which lysed the cells and increased the possibility of cell rupture (Huang *et al.* 2021). The EDTA method had the lowest polysaccharide content, and the protein content was only 0.07 mg/L higher than the NaOH method. Liu & Fang (2002) suggested that there was formation of complexes between EDTA and the EPS. These

Table 2 | The total amount of EPS and the content of each component using different extraction methods

Extraction method	Total EPS (mg/L)	Protein (mg/L)	Polysaccharide(mg/L)
Ultrasonic	68.95	14.50	54.45
Heating	68.77	14.02	54.75
EDTA	57.65	12.51	45.14
NaOH	62.61	12.44	50.17

EDTA-EPS complexes were not removed by membrane separation and thus the EDTA remained in the EPS. Chemical extraction EPS will be contaminated by chemical reagents which may affect the determination of EPS components.

In the subsequent experiments, EPS was extracted by ultrasonic method. The EPS concentration was 68.95 mg/L, which was used as the basis for the EPS dosage in the adsorption test.

3.2. Mechanism of EPS adsorption Th^{4+}

3.2.1. FTIR spectra analysis

The functional groups in EPS are a significant factor that influences Th^{4+} adsorption (Tang *et al.* 2021). The FTIR spectra of EPS before and after Th^{4+} adsorption is illustrated in Figure 4. From an overall perspective, the profiles of FTIR spectra for the EPS before and after Th^{4+} adsorption were similar, suggesting that their chemical groups are similar. However, some differences in the peaks can be found after careful comparison of the FTIR spectra. Firstly, the EPS showed the changes after Th^{4+} adsorption, that is, the peak at 3279 cm^{-1} changed, implying a possible interaction between Th^{4+} and C–H from methyl and methylene. Secondly, for EPS, the respective intensity of the peaks at about 1631 and 1532 cm^{-1} was found to decrease after Th^{4+} adsorption. This indicated that amide I and amide II of proteins played a crucial role during Th^{4+} adsorption. Additionally, the bands ranging from 1387 to 1227 cm^{-1} changed irregularly after Th^{4+} bonding. This implied that those aliphatic C–H stretching vibration and O–H and C = O related carboxylic acid also made a great contribution to Th^{4+} adsorption. Combining with the variations in functional groups of EPS extracted by ultrasonic method from tailing observed above, it was deduced that amide I and amide II of proteins, C–H from aliphatic, as well as O–H and C–O from carboxylic acid, play the significant role in Th^{4+} adsorption. These functional groups in EPS could coordinate with Th^{4+} to form chelates, thereby removing Th^{4+} in aqueous solution (Tang *et al.* 2021).

3.2.2. 3D-EEM analysis

The fluorescence changes of EPS before and after adsorption are shown in Figure 5. It can be seen from Figure 5 that peak A and peak D are tryptophan-like fluorescent substances located at Ex/Em = 280/325 nm, Ex/Em = 285/345 nm while peak B is a tyrosine-like fluorescent substance located at Ex/Em = 230/320 nm. Both of them are fluorescent proteins, because of the aromatic cyclic amino acids in EPS (Guo *et al.* 2014). Peak C is a humic acid-like substance located at Ex/Em = 337/416 nm. The results of the study showed that the extracted EPS mainly consisted of tryptophan and tyrosine-based proteins. Since tryptophan and tyrosine are hydrophobic amino acids with strong hydrophobic side chains that provide hydrophobic adsorption sites mainly on EPS, this allows Th^{4+} to bind tightly to EPS. Previously published studies have shown that the fluorescence intensity is closely related to the content of EPS (Ma *et al.* 2018). It can be seen from the figure that the fluorescence intensity of tryptophan after adsorption was significantly weakened and the EPS content was reduced. The above

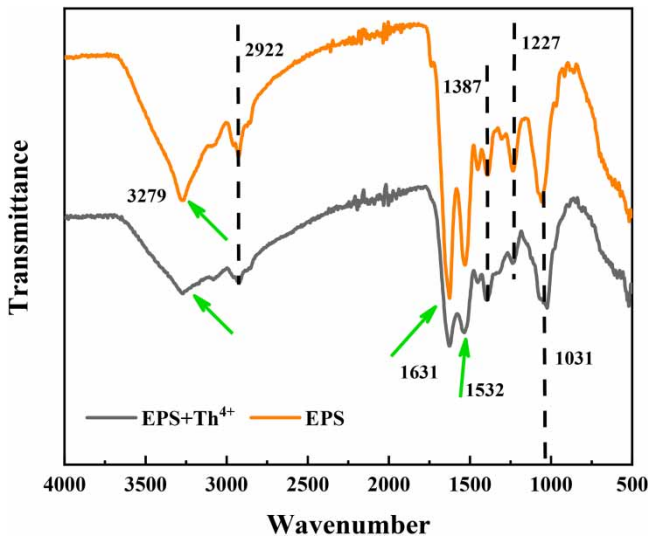

Figure 4 | FTIR spectra before and after Th^{4+} adsorption.

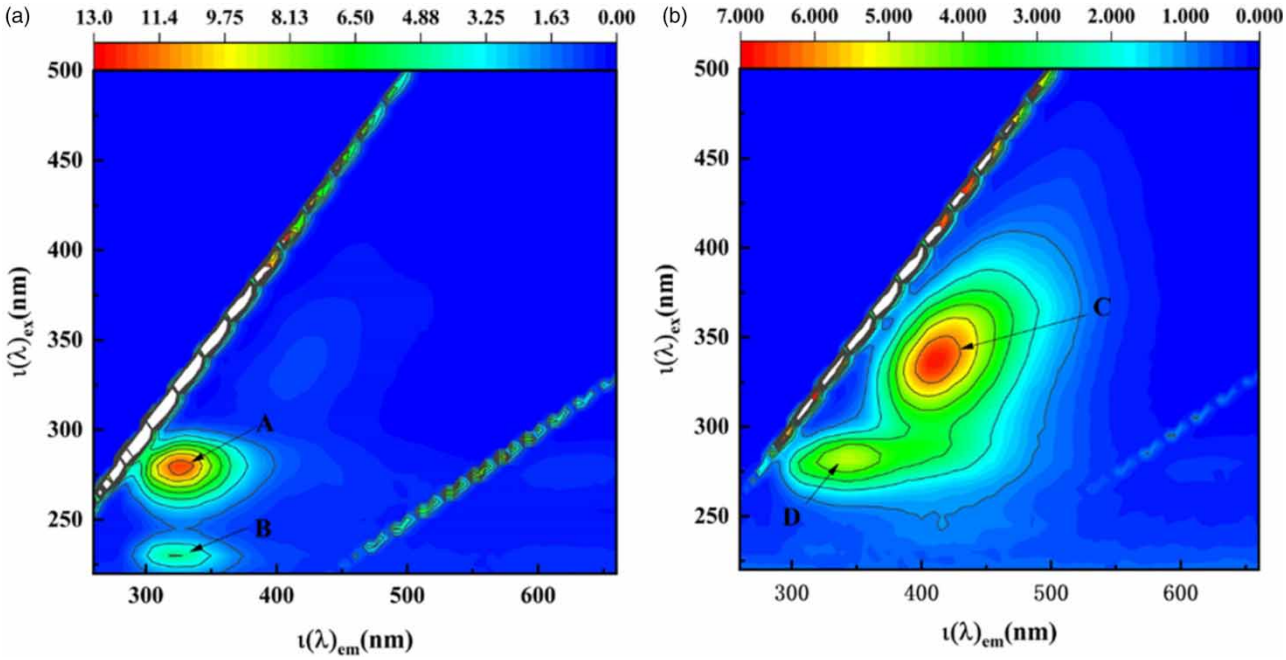

Figure 5 | 3D-EEM before (a) and after (b) Th^{4+} adsorption.

results indicate that protein is the main component of EPS and plays an important role in the adsorption process. In addition, some humus-like substances have increased slightly.

3.2.3. Effect of pH on adsorption of Th^{4+} by EPS

The pH value is one of the most significant environmental factors influencing not only site dissociation, but also the speciation and the biosorption availability of heavy metals (Özer *et al.* 2004). The variation of removal efficiency and adsorption capacities with the pH is shown in Figure 6. The adsorption increases with increasing pH and reaches a maximum ($R = 78.01\%$; $q_e = 26.6926$ mg/g) at pH = 3.5. At pH < 3.5, the surface of EPS would be surrounded by H_3O^+ ions which compete with Th^{4+} for the adsorption sites and decrease the Th^{4+} interaction with binding sites of the surface of EPS by greater repulsive forces (Özer *et al.* 2004). As pH increases, the acidity of the solution decreases while the number of

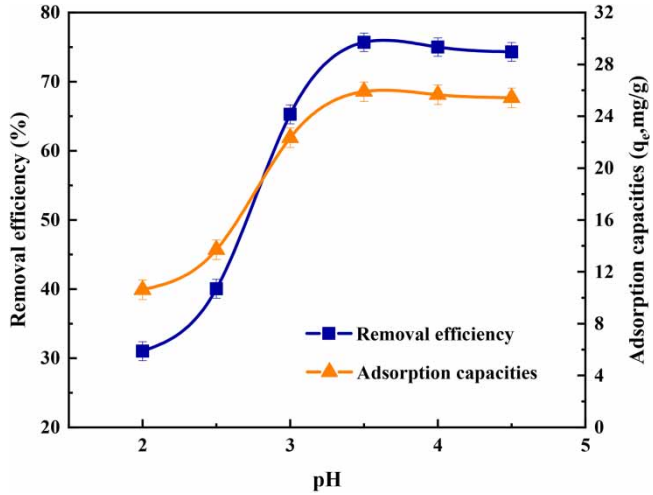

Figure 6 | Effect of different pH on Th^{4+} removal (Th^{4+} concentration = 20 mg/L; reaction time = 15 h; EPS dosage = 30 mL).

binding sites increases, and therefore, the adsorption of Th^{4+} increases. At pH>3.5, the metal ions combine with various anions in the solution to form negatively charged groups, which are not easy to combine with the adsorption site. The results showed that the optimal pH for Th^{4+} to be adsorbed was 3.5.

3.2.4. Effect of initial concentration of Th^{4+}

The removal efficiency and adsorption capacities for Th^{4+} adsorption onto EPS are given in Figure 7 as a function of the initial Th^{4+} concentrations. As seen in Figure 7, the adsorption capacities increased with increasing initial Th^{4+} concentrations as a result of the increase in the driving force. The removal efficiency of Th^{4+} adsorption by EPS decreased from 84.02 to 70.13% as the initial Th^{4+} concentration was increased from 10 to 50 mg/L. At lower Th^{4+} concentrations, all Th^{4+} present in the solution could interact with the binding sites and thus the removal efficiency was higher than those at higher initial Th^{4+} concentrations. At higher concentrations, lower removal efficiency is due to the saturation of adsorption sites. As an experiment result, the available sites on the surface of EPS are the limiting factor for Th^{4+} adsorption. Considering that the initial concentration of Th^{4+} is 20 mg/L, its removal effect is great, therefore this concentration is used for subsequent experiments.

3.2.5. Effect of EPS dosage

The EPS dosage was investigated at 25 °C over the range (10 ~ 60 mL). As shown in Figure 8, in terms of overall changes, with the increase in EPS dosage, the Th^{4+} removal efficiency increased, and the adsorption capacities of EPS decreased. The removal efficiency of Th^{4+} increases from 39.58 to 76.15% with raising the EPS dosage from 10 to 60 mL. It could be ascribed to the larger amount of adsorption sites provided by the increasing EPS dosage. By contrast, the adsorption capacities of the EPS decreased from 46.43 to 13.97 mg/g with the increasing EPS dosage. This is because with the increase in the amount of adsorbent, the polymer chain structure of the adsorption site was embedded and did not play the adsorption role (Zheng 2008). In addition, the strength of the binding site on the surface of the adsorbent is different, so the competitive adsorption of metal ions between the adsorbents will also lead to the reduction of the unit adsorption capacity.

Notably, when the EPS is 30 mL, the Th^{4+} removal efficiency curve has an inflection point. Before this inflection point, the Th^{4+} removal efficiency increased with the increase in EPS dosage. After this inflection point, the increase in the EPS dosage did not obviously increase the Th^{4+} removal efficiency. Thus, 30 mL as best dosing quantity was applied in the subsequent experiments.

3.2.6. Effect of reaction time

The changes in removal efficiency of Th^{4+} with reaction time are shown in Figure 9. The process of Th^{4+} removal and Th^{4+} adsorption by EPS could be divided into three stages. In the first rapid adsorption stage (0 ~ 2 h), the removal efficiency of EPS quickly increased to 36.3%. This phenomenon indicated that the utilization of the abundant binding sites on the surface

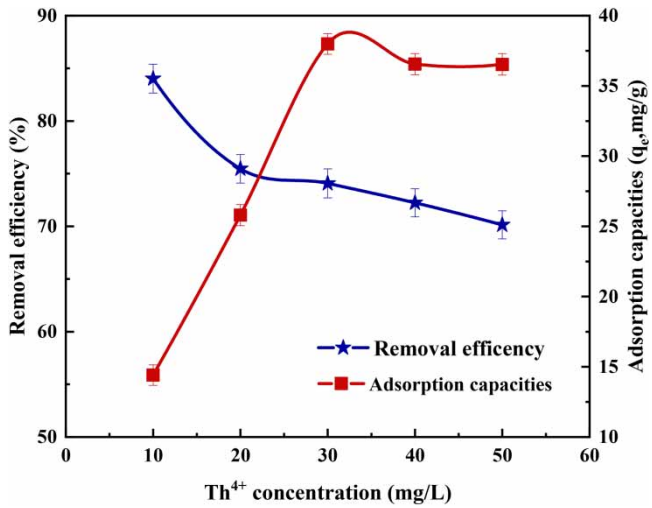

Figure 7 | Effect of Th^{4+} initial concentration on Th^{4+} removal (pH = 3.5; reaction time = 15 h; EPS dosage = 30 mL).

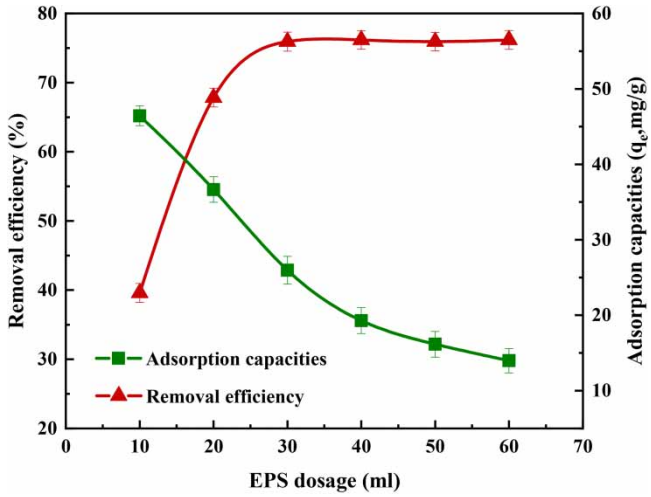

Figure 8 | Effect of EPS dosage on Th^{4+} removal (Th^{4+} concentration = 20 mg/L; reaction time = 15 h; pH = 3.5).

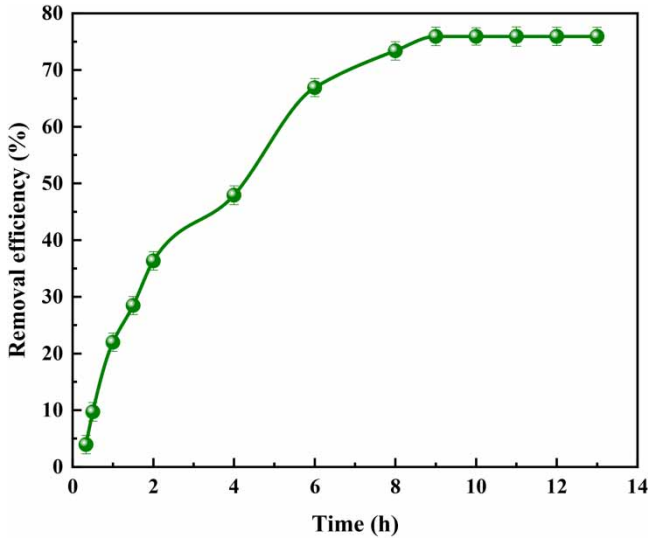

Figure 9 | Effect of contact time on removal efficiency (Th^{4+} concentration = 20 mg/L; pH = 3.5; EPS dosage = 30 mL).

of EPS to adsorb Th^{4+} was extremely rapid. In the second slow adsorption stage (2 ~ 9 h), the Th^{4+} removal rate slowly increased to 75.46%. In the third stage of adsorption equilibrium (9 ~ 13 h), the Th^{4+} removal efficiency of EPS basically no longer increased.

3.2.7. Adsorption isotherms of EPS

Langmuir isotherm model is mainly used to study the maximum monolayer adsorption Freundlich isotherm model is usually better to describe the adsorption in aqueous solution (Xiong *et al.* 2009).

The Th^{4+} adsorption isotherms of EPS were described by classical Langmuir and Freundlich models.

The linear and nonlinear expressions of the Langmuir isotherm are as follows:

$$\frac{C_e}{q_e} = \frac{C_e}{q_{\max}} + \frac{1}{bq_{\max}} \quad \text{(linear)} \tag{3}$$

$$q_e = \frac{bC_e q_{\max}}{1 + bq_{\max}} \quad \text{(non-linear)} \tag{4}$$

where C_e is the equilibrium concentration of Th^{4+} (mg/L) in solution, q_e is the amount of Th^{4+} adsorbed at equilibrium, mg/g, q_{max} is the theoretical maximum adsorption capacity, mg/g, b is a constant related to the energy or net enthalpy of adsorption, L/mg.

The linear and nonlinear expressions of the Freundlich isotherm are as follows:

$$\ln q_e = \ln k + \ln C_e \quad \text{(linear)} \tag{5}$$

$$q_e = kC_e^{\frac{1}{n}} \quad \text{(non-linear)} \tag{6}$$

where k and n are Freundlich constants representing adsorption capacity (L/mg) and adsorption intensity, respectively. The values of $1/n$ between 0 and 1 suggest favorable adsorption (Hamane *et al.* 2015).

Experiments were performed at different temperatures (15, 25, and 30 °C) at a Th^{4+} concentration of 20 mg/L, EPS dosage of 30 mL at pH = 3.5, and a contact time of 15 h. The linearized and non-linearized Langmuir and Freundlich adsorption isotherms of Th^{4+} obtained are given in Figure 10. The evaluation of the isotherms at different temperatures with the correlation coefficients is also presented in Table 3. Comparing the correlation coefficients, it can be concluded that the Langmuir

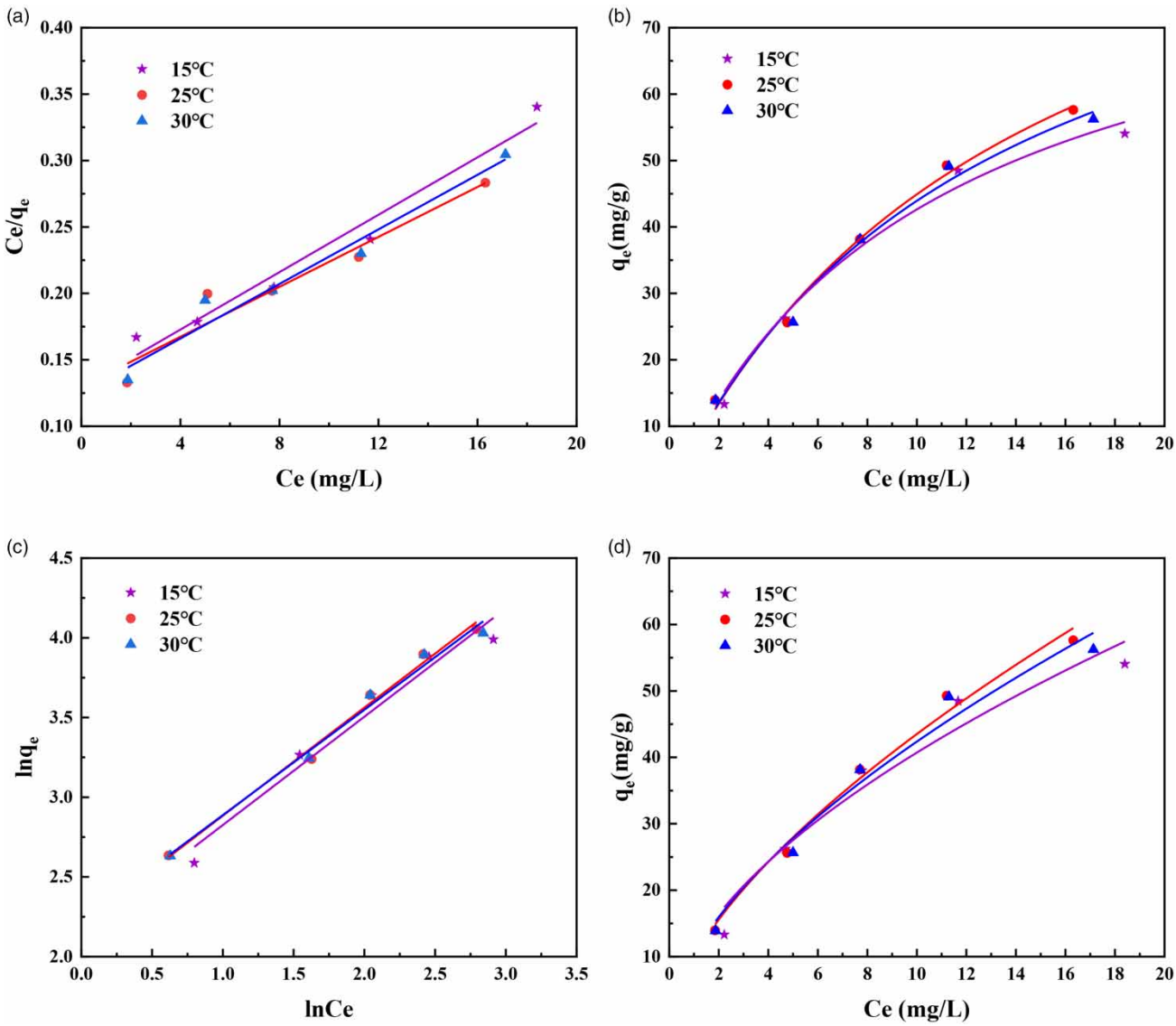

Figure 10 | Linear (a) and non-linear (b) of Langmuir adsorption isotherm models, linear (c) and non-linear (d) of Freundlich adsorption isotherm models.

Table 3 | Linear and non-linear fitting parameters of Langmuir and Freundlich adsorption isotherm models

		Langmuir			Freundlich		
Type	θ/°C	b/(L/mg)	q_{max}/(mg/g)	R^2	k/(L/g)	$\frac{1}{n}$	R^2
Linear	15	0.270 ± 0.0121	28.811 ± 0.00141	0.9676	8.552 ± 0.159	0.651 ± 0.0767	0.9632
	25	0.256 ± 0.0139	30.129 ± 0.0012	0.9364	9.0823 ± 0.0088	0.632 ± 0.0432	0.9903
	30	0.658 ± 0.0118	31.219 ± 0.0014	0.9627	9.273 ± 0.0791	0.661 ± 0.0388	0.9873
Non-linear	15	0.0937 ± 0.0169	28.147 ± 0.0870	0.9875	11.109 ± 0.122	0.952 ± 0.0499	0.9883
	25	0.0698 ± 0.117	30.927 ± 0.0134	0.9944	10.0161 ± 0.177	0.0379 ± 0.0685	0.9754
	30	0.0781 ± 0.0187	30.224 ± 0.118	0.9887	10.472 ± 0.241	0.607 ± 0.0868	0.9524

and Freundlich isotherms fit the experimental data better for the considered adsorption system. This indicates that in the adsorption process, there is a certain van der Waals force between EPS and Th^{4+} and the physical adsorption occurs in monolayer molecules on the surface of EPS. The $1/n$ calculated by the Freundlich equation were between 0 and 1, confirming the adsorption of Th^{4+} onto the EPS was favorable. The k value reflects the affinity of the adsorption system with metal ions. The k value of $8.55 \sim 11.11$ indicates EPS has a strong affinity for Th^{4+} in the aqueous environment (Wang *et al.* 2008).

The better adsorption capacity of Th^{4+} might be due to the presence of various functional groups at the surface of EPS which can attach to Th^{4+} via physicochemical interactions. This also confirms the conclusion obtained by FTIR spectral analysis in section 3.2.1.

In order to further explore the thermodynamic mechanism of EPS adsorption on Th^{4+}, the adsorption process was analyzed. The thermodynamic parameters: free energy (ΔG), enthalpy (ΔH), and entropy (ΔS) change of Th^{4+} adsorption are evaluated from the following equations:

$$K_0 = q_{\max} \times b \tag{7}$$

$$\ln K_0 = -\frac{\Delta H}{R} \times \frac{1}{T} + \frac{\Delta S}{R} \tag{8}$$

$$\Delta G = -RT\ln K_0 \tag{9}$$

$$\Delta S = \frac{\Delta H - \Delta G}{T} \tag{10}$$

where K_0 is the distribution coefficient for adsorption, L/g; R is the universal gas constant, 8.314 J/(mol·K); T is the absolute temperature, K. ΔS and ΔH are deduced from the intercept and slope of the linear plot of $\ln K_0$ versus $1/T$.

The parameters ΔG, ΔS and ΔH are listed in Table 4.

It can be seen from Table 3 that the Th^{4+} adsorption increases slightly from 28.81 to 31.22 mg/g with increasing temperature from 15 to 30 °C, indicating an endothermic process. Also, the positive value of ΔH confirms the heat-absorbing nature of EPS adsorption and the negative ΔG at different temperatures indicates spontaneous adsorption. Furthermore, the decrease of ΔG with an increasing temperature suggests that the adsorption is more favorable at higher temperatures. The positive value of ΔS indicates that the confusion degree of the system increases, reflecting the affinity of EPS for Th^{4+}.

From the perspective of energy conservation, all experiments were carried out at 25 °C.

Table 4 | Thermodynamics parameters for the adsorption of Th^{4+} by EPS

T/K	ΔG/(kJ/mol)	ΔH/(kJ/mol)	ΔS/[J/(mol·K)]
288	−4.914		
298	−5.065	39.381	152.669
303	−7.613		

3.2.8. Adsorption kinetics of EPS

Pseudo-first-order, and pseudo-second-order kinetic equations were used to conduct the adsorption kinetics of EPS in the sorption process to analyze the adsorption mechanism.

The linear and nonlinear expressions of the pseudo-first-order dynamics model are as follows:

$$\ln(q_e - q_t) = \ln q_e - \frac{k_1 t}{2.303} \quad \text{(linear)} \tag{11}$$

$$q_t = q_e(1 - e^{-k_1 t}) \quad \text{(non-linear)} \tag{12}$$

where q_e and q_t are the amounts of Th^{4+} adsorbed at equilibrium and at time t, respectively, mg/g. k_1 is the pseudo-first-order rate constant, 1/h.

The linear and nonlinear expressions of the pseudo-second-order dynamics model are as follows:

$$\frac{t}{q_t} = \frac{1}{k_2 q_e^2} + \frac{t}{q_e} \quad \text{(linear)} \tag{13}$$

$$q_t = \frac{k_2 q_e^2 t}{1 + k_2 q_e t} \quad \text{(non-linear)} \tag{14}$$

where k_2 is the pseudo-second order rate constant, mg/(g · h).

The fitting results are listed in Table 5 and illustrated in Figure 11. The correlation coefficients (R^2) of the pseudo-second-order equation closed to 1, while that of the pseudo-first-order equation was low. The calculated q_e (33.047 mg/g) values in the case of the pseudo-second-order equation also agreed with the experimental data. These results indicated that the EPS adsorption system is well described by the pseudo-second-order model, based on the assumption that the rate-limiting step may be chemisorption involving valency forces through sharing or exchange of electrons between adsorbent and adsorbate (Özer *et al.* 2004). This is similar to the results of the study by Xu *et al.* (2021). And the polysaccharides content in EPS is higher than proteins, which indicates that the adsorption rate of polysaccharides in EPS is faster than that of proteins.

The adsorbate species are most probably transported from the bulk of the solution into the solid phase through intra-particle diffusion/transport process, which is often the rate-limiting step in many adsorption processes (Özer *et al.* 2004). In order to further study the rate limiting steps of EPS adsorption behavior on Th^{4+}, the intra-particle diffusion of Th^{4+} adsorption by EPS was explored by using the intra-particle diffusion model. The intra-particle diffusion equation is as follow:

$$q_t = k_3 t^{\frac{1}{2}} + c \tag{15}$$

where k_3 is the diffusion rate constant in particles, g/(mg·h$^{\frac{1}{2}}$); C is the diffusion constant within the particle, g/(mg·h$^{\frac{1}{2}}$).

The intra-particle diffusion equation was used to fit the data of EPS adsorption of Th^{4+}, the results are shown in Figure 12. It can be seen from Figure 12 that EPS adsorption process of Th^{4+} can be divided into three stages according to the intra-particle diffusion process, and the slope k_3 of the three stages decreases with the increase of time, indicating that the adsorption amount gradually decreases and finally reaches equilibrium. The previous research has shown that if the intra-particle diffusion is the sole rate limiting step, it is essential for the plot q_t versus $t^{\frac{1}{2}}$ to pass by the origin, which is not the case in this experiment (Özer *et al.* 2004). The plots present multi-linearity, this indicates the intra-particle diffusion involved in the Th^{4+} adsorption by EPS, but is not the sole rate-controlling-step.

Table 5 | Parameters of linear and non-linear pseudo-first-order kinetics and pseudo-second-order kinetics

	Pseudo-first-order kinetics			Pseudo-second-order kinetics		
Type	q_e/(mg/g)	k_1/h	R_1^2	q_e/(mg/g)	k_2/(g/mg·h)	R_2^2
Linear	28.416 ± 0.152	0.230 ± 0.0201	0.9425	33.047 ± 0.0097	0.0099 ± 0.0013	0.9825
Non-linear	27.547 ± 0.753	0.277 ± 0.0241	0.9895	33.787 ± 0.568	0.00918 ± 0.0003	0.9837

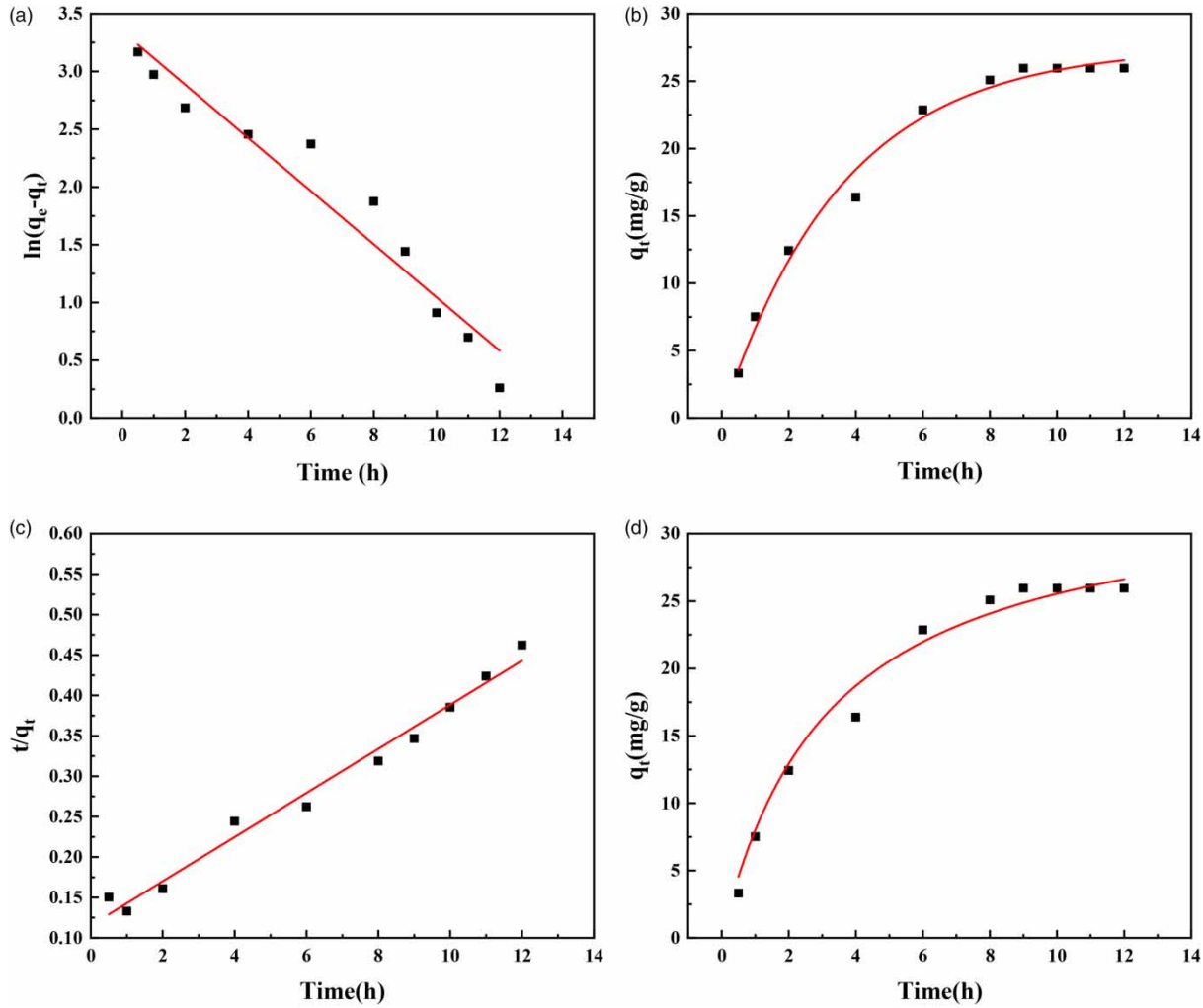

Figure 11 | A Linear (a) and non-linear (b) of pseudo-first-order kinetic models, linear (c) and non-linear (d) of pseudo-second-order kinetic models.

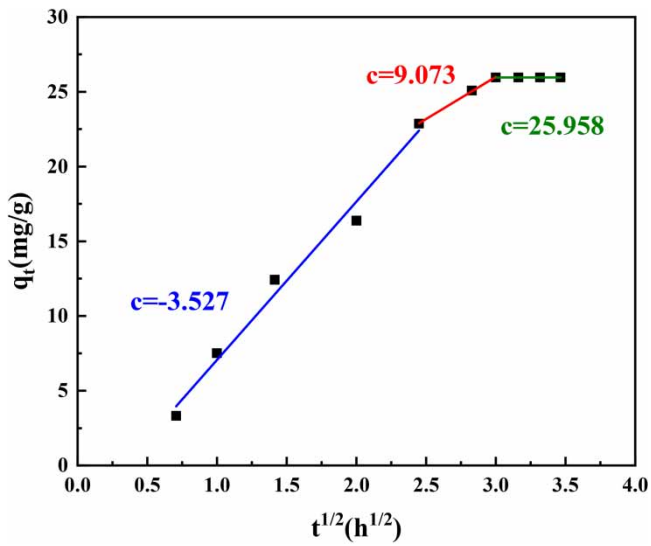

Figure 12 | Fitting curves for intra-particle diffusion of EPS adsorbed Th^{4+}.

4. CONCLUSIONS

1. The ultrasonic extraction method has the best effect on extracting EPS from indigenous bacteria of rare earth tailings, and the physical extraction method is generally more efficient than the chemical extraction method.
2. The key factor of EPS adsorbed Th^{4+} was functional groups, including amide I and amide II of proteins, C–H from aliphatic, as well as O–H and C = O from carboxylic acid.
3. The hydrophobic interaction of tryptophan and tyrosine in EPS plays an important role in the adsorption process.
4. The pH, initial Th^{4+} concentration, and EPS dosage affected the equilibrium uptake of Th^{4+} to EPS, and the optimum pH, initial Th^{4+} concentration, and EPS dosage were determined as 3.5, 20 mg/L, and 30 mL, respectively.
5. An increase in the adsorption of Th^{4+} deals with increasing temperature up and then followed by an exothermic uptake process at higher temperatures.
6. The Langmuir and Freundlich adsorption models were applied to describe the experimental data. Equilibrium data fitted very well to both the Langmuir and Freundlich isotherm models.
7. The kinetic data adsorption of EPS to Th^{4+} was found to follow the pseudo-second-order model. Chemical adsorption is the main adsorption mechanism.

ACKNOWLEDGEMENTS

The authors wish to thank the Natural Science Foundation of Inner Mongolia Autonomous Region of China (No. 2020MS02015, No. 2020MS0547), the National Natural Science Foundation of China (No. 42167029), the Open Program of Tianjin Key Laboratory of Green Chemical Engineering Proceed Engineering of Tianjin University (GCEPE20190108) for their support of this study.

DECLARATION OF COMPETING INTEREST

The authors declare that they have no known competing financial interests or personal relationships that could have appeared to influence the work reported in this paper.

DATA AVAILABILITY STATEMENT

All relevant data are included in the paper or its Supplementary Information.

CONFLICT OF INTEREST

The authors declare there is no conflict.

REFERENCES

Cadena, D. G. 1983 Limits for intakes of radionuclides by workers. ICRP publication 30, part 3. *Medical Physics* **10** (6), 919–919.

Chen, J. Y., Fan, H. H., Meng, Y. N. & Wang, S. Y. 2022 Geochemical properties and resource distribution of thorium. *Journal of University of South China (Science and Technology)* **36** (01), 52–57.

Comte, S., Guibaud, G. & Baudu, M. 2006 Relation between extraction protocols of the activated sludge extracellular polymeric substances(EPS) and EPS complexation properties. Part I: comparison of the efficiency of eight EPS extraction properties. *Enzyme Microbial Technology* **38**, 237–245.

Guo, P. P., Yu, H. Q. & Li, X. Y. 2010 Extracellular polymeric substances (EPS) of microbial aggregates in biological wastewater treatment systems: a review. *Biotechnology Advances* **28** (2010), 882–894.

Guo, X. J., He, L. S., Li, Q., Yuan, D. H. & Deng, Y. 2014 Investigating the spatial variability of dissolved organic matter quantity and composition in Lake Wuliangsuhai. *Ecological Engineering* **62**, 93–101.

Gupta, P. & Batul, D. 2016 Bacterial exopolysaccharide mediated heavy metal removal: a review on biosynthesis, mechanism and remediation strategies. *Biotechnology Reports* **13**, 58–71.

Hamane, D., Arous, O., Kaouah, F., Trari, M., Kerdjoudj, H. & Bendjama, Z. 2015 Adsorption/photo-electrodialysis combination system for Pb^{2+} removal using bentonite/membrane/semiconductor. *Environmental Chemical Engineering* **3** (2015), 60–69.

Han, J. H., Song, Y. Y., Zhang, T. J., Jiang, Q. H., Zhang, L. K. & Wang, W. D. 2020 Screening and identification of Cr(VI) reducing bacteria. *Microbiology China* **47** (10), 3206–3215.

Huang, R. X., He, Q., Ma, J., Ma, C. X., Xu, Y. H., Song, J. H., Sun, L. L., Wu, Z. S. & Huangfu, X. L. 2021 Quantitative assessment of extraction methods for bound extracellular polymeric substances (B-EPSs) produced by *Microcystis sp.* and *Scenedesmus sp*. *Algal Research* **56** (2021), 102289.

Kang, D. J., Xie, D. Y., Kuang, S., Jiang, X., Sun, J., Tang, H. & Fu, F. F. 2016 Adsorption mechanism of extracellular polymeric substances in activated sludge on Pb^{2+} and Cu^{2+}. *China Water &Wastewater* **21**, 28–33.

Li, X. Y. & Yang, S. F. 2007 Influence of loosely bound extracellular polymeric substances (EPS) on the flocculation, sedimentation, and dewaterability of activated sludge. *Water Research* **41** (2007), 1022–1030.

Li, J., Wang, X. X., Zhao, G. X., Chen, C. L., Chai, Z. F., Ahmed, A., Tasawar, H. & Wang, X. K. 2018 Metal-organic framework-based materials: superior adsorbents for the capture of toxic and radioactive metal ions. *Chemical Society Reviews* **47** (7), 2322–2356.

Liu, H. & Fang, H. H. P. 2002 Extraction of extracellular polymeric substances (EPS) of sludges. *Biotechnology* **95**, 249–256.

Ma, B., Li, S., Wang, S., Gao, M., Guo, L., She, Z., Zhao, Y., Jin, C., Yu, N. & Zhao, C. 2018 Effect of Fe_3O_4 nanoparticles on composition and spectroscopic characteristics of extracellular polymeric substances from activated sludge. *Process Biochemistry* **75**, 212–220.

More, T. T., Yadav, J. S. S., Yan, S., Tyagi, R. D. & Surampalli, R. Y. 2014 Extracellular polymeric substances of bacteria and their potential environmental applications. *Environmental Management* **144**, 1–25.

Nouha, K., Kumar, R. S. & Tyagi, R. D. 2016 Heavy metals removal from wastewater using extracellular polymeric substances produced by Cloacibacterium normanense in wastewater sludge supplemented with crude glycerol and study of extracellular polymeric substances extraction by different methods. *Bioresource Technology* **212**, 120–129.

Özer, A., Özer, D. & EkÌz, H. Ì. 2004 The equilibrium and kinetic modeling of the biosorption of copper(II) ions on Cladophora crispata. *Adsorption: The International Adsorption Society* **10** (4), 317–326.

Tang, C. J., Chen, X., Feng, F., Liu, Z. G., Song, Y. X., Wang, Y. Y. & Tang, X. 2021 Roles of bacterial cell and extracellular polymeric substance on adsorption of Cu(II) in activated sludges: a comparative study. *Water Process Engineering* **41** (2021), 102094.

Wang, B. E., Hu, Y. Y. & Xie, L. 2008 Mechanism of reactive brilliant blue KN-R by inactive aspergillus fumigatus immobilized on CMC beads: equilibrium kinetics diffusion and mass transfer. *Acta Scientiae Circumstantiae* **28** (1), 89–84.

Wang, J., Li, Q., Li, M. M., Chen, T. H., Zhou, Y. F. & Yue, Z. B. 2014 Competitive adsorption of heavy metal by extracellular polymeric substances (EPS) extracted from sulfate reducing bacteria. *Bioresource Technology* **163**, 374–376.

Wei, L. L., Li, Y., Daniel, R. N., Zhao, N. B., Song, Y., Ding, J., Zhao, Q. L. & Cui, F. Y. 2016 Adsorption of Cu^{2+} and Zn^{2+} by extracellular polymeric substances (EPS) in different sludges: effect of EPS fractional polarity on binding mechanism. *Hazardous Materials* **321**, 473–483.

Xiao, R. & Zheng, Y. 2016 Overview of microalgal extracellular polymeric substances (EPS) and their applications. *Biotechnology Advances* **34** (2016), 1225–1244.

Xiong, F., Hu, Y. & Yin, Y. R. 2009 Biosorption of Pb^{2+} by extracellular polymeric substances produced by aspergillus fumigatus. *Acta Scientiae Circumstantiae* **29** (11), 2289–2294.

Xu, G. X., Shi, C. X., Wang, D. Z., Zhao, Z. X., Wang, D. Z., He, Z. X., Wang, N. Y., Fang, S. X., Guo, M. S., Ou, Y. Y., Fei, W. Y., Liu, Y. F., Yang, Y. C., Li, D. Y., Tang, X. Y. & Gu, Z. M. 2005 Urgent appeal for the protection of thorium and rare earth resources in bayan Obo mine from radioactive contamination in the Yellow River and Baotou. *Bulletin of Chinese Academy of Sciences* **20** (6), 448–450.

Xu, X. H., Wei, D. Z. & Zhang, L. H. 2021 Extraction and adsorption properties of extracellular polymeric substance. *Journal of Northeastern University (Natural Science)* **10** (2021), 1468–1474.

Yang, S. K., Wu, W. L. & Hou, X. J. 2017 Sorption of thorium(IV) from aqueous solutions by melamine modified lemna minor. *Acta Scientiae Circumstantiae* **37** (4), 1413–1418.

Zhang, S. J., Xu, C. & Peter, H. S. 2008 Chemical composition and 234 Th (IV) binding of extracellular polymeric substances (EPS) produced by the marine diatom *Amphora sp*. *Marine Chemistry* **112** (1–2), 81–92.

Zhao, H. J., Zhong, C. Y., Chen, H. G., Yao, J., Tan, L. Q., Zhang, Y. L. & Zhou, J. G. 2016 Production of bioflocculants prepared from formaldehyde wastewater for the potential removal of arsenic. *Environmental Management* **172**, 71–76.

Zheng, Y. 2008 *Production of Purifying Agent and Its Use in Treatment of Heavy Metal and Suspension Wastewater*. Ph.D. Thesis, Shanghai Jiao Tong University, Shanghai, China, pp. 96–97.

Zhou, Y., Binh, T. N., Lai, Y. J. S., Zhou, C., Xia, S. Q. & Bruce, E. R. 2016 Using flow cytometry to evaluate thermal extraction of EPS from *Synechocystis sp.* PCC 6803. *Algal Research* **20** (2016), 276–281.

First received 11 July 2022; accepted in revised form 11 December 2022. Available online 17 December 2022